Supporting Information

Carbon Dots from Alcohol Molecules: Principles and Reaction Mechanism

Hanyu Tu, Huaxin Liu, Laiqiang Xu, Zheng Luo, Lin Li, Ye Tian, Wentao Deng, Guoqiang Zou, Hongshuai Hou* and Xiaobo Ji*

State Key Laboratory of Powder Metallurgy, College of Chemistry and Chemical Engineering, Central South University, Changsha, 410083, China

Corresponding Author

Hongshuai Hou, Xiaobo Ji

E-mail: hs-hou@csu.edu.cn; xji@csu.edu.cn

1. Experimental Procedures

1.1 Synthesis of carbon dots

The 100EA-CDs were obtained by electrochemical synthesis method. Specifically, 8 g sodium hydroxide (NaOH) were dissolved in 100 mL ethanol (CH_3CH_2OH) under constant stirring, and then 20 V DC voltage was applied to the mixture with two Pt sheets as the electrodes. After that, the reaction solution was cooled down to the room temperature naturally. Then, the CDs purification was further performed to be neutral by dialyzing in a dialysis bag for 5 days, followed by freeze-drying to obtain brown powder. For the synthesis of 90EA-CDs, 80EA-CDs, 60EA-CDs, 50EA-CDs, 100EG-CDs, 80EG-CDs, 100GL-CDs, 80GL-CDs, and 100NBA-CDs, 90 mL CH_3CH_2OH and 10 mL H_2O, 80 mL CH_3CH_2OH and 20 mL H_2O, 60 mL CH_3CH_2OH and 40 mL H_2O, 50 mL CH_3CH_2OH and 50 mL H_2O, 100 mL ethylene glycol ($C_2H_6O_2$), 80 mL $C_2H_6O_2$ and 20 mL H_2O, 100 mL glycerol ($C_3H_8O_3$), 80 mL $C_3H_8O_3$ and 20 mL H_2O, 100 mL n-butanol ($CH_3CH_2CH_2CH_2OH$) were utilized as electrolyte solution, respectively. 8 g NaOH were dissolved in each electrolyte under constant stirring and 20 V DC voltage was applied to the mixture. Next purification steps were the same as 100EA-CDs.

1.2 Synthesis of NVP cathode

The $Na_3V_2(PO_4)_3$ (NVP) cathode was prepared according to previous report.[1] Next, cathode plate was acquired by mixing 80 wt% pre-prepared NVP, 10 wt% binder polyvinylidene fluoride (PVDF), and 10 wt% conductive carbon (Super P) in N-methyl pyrrolidinone (NMP). The well-mixed slurry was coated onto Al foil and further dried under vacuum at 120 °C for 12 h. The diameters of cathode, separator, and anode in a full cell are 12mm, 19mm, 15mm, respectively. The areal mass loading of the active material was ~2.5 mg cm^{-2}. 80 μL of electrolyte was supplied in each cell.

1.3 Characterizations

The microstructural and surface state of CDs were characterized by typical transmission electron microscopy (TEM) (FEI Tecnai F20), X-ray diffraction (XRD) (Rigaku Ultima IV), X-ray photoelectron spectroscopy (XPS) (Thermo Scientific K-Alpha) and Fourier transform infrared spectroscopy (FTIR) (Thermo Scientific Nicolet iS20), UV/Vis absorbance spectroscopy (UV-2600), respectively. The electrolyte solution was analyzed on an TRACE1300-ISQ7000 gas chromatography-mass spectrometry. The column used for separa-tion was a HP-5MS column (30 m×0.25 mm, 0.25 μm). The morphology of Na^+ ions deposition with and without Na-CDs added were characterized by scanning transmission electron microscopy (SEM) (JEOL/JSM-7610FPlus). In detail, the coin cells after different cycles were disassembled in the Ar-filled glove box and then the electrodes were rinsed to remove the residual electrolyte solute by 1,2-dimethoxyethane (DME) before observation. Raman spectroscopy measurement were conducted on Horiba LabRAM HR Evolution.

1.4 Electrochemical measurements

In an Ar-filled glove box (O_2<0.01 ppm, H_2O<0.01 ppm), the CDs powders were dispersed into conventional electrolyte (1.0 M $NaPF_6$ in DIGLYME). All of the electrochemical performance tests were carried out at room temperature and using standard CR2016-type coin cells on battery testing system (LAND, Wuhan, China). The Na∥Cu half-cells were assembled with sodium foil anode as well as copper foil cathode for coulombic efficiency testing and then the Na∥Cu half-cells were cycled within a voltage range of 0 to 1.0 V (vs. Na^+/Na) at current densities of 0.5 and 1.0 mA cm^{-2}. As for long-term cycling, the Na∥Na symmetric-cells were assembled with two sodium foils and then tested at the current densities of 0.5, 1.0, 2.0, 3.0 and 5.0 mA cm^{-2} with an areal capacity of 1.0 mAh cm^{-2}. Besides, Na∥NVP full-cells were assembled with as-prepared NVP cathode and sodium anode and were tested within a voltage range of 2.5 to 3.8 V (vs. Na^+/Na) at rate of 1.0, 5.0, 10.0, 15.0, and 20.0 C (1.0 C=117 mA g^{-1}). Moreover, the electrochemical impedance spectroscopy (EIS) was tested on Autolab (MULTI AUTOLAB M204) electrochemical workstation with a frequency range from 10^{-2} to 10^5 Hz.

1.5 Computational methods

Density functional theory (DFT) calculation was carried out with the Dmol3 module as implemented in the Materials Studios package of Accelrys Inc to obtain the binding energy between Na ions with each sodiophilic site. For all calculations, each geometries of the Na ions with Na-CDs bonded were optimized until the energyand force convergence criteria are 2.0 x 10^{-5} Ha and 0.004 Ha A^{-1}, respectively. Thereinto, the binding energy was defined as E(Na-CDs-Na^+)-E(Na-CDs)-E(Na^+), and it was calculated with the basis set superpositionerror corrected by the counterpoise method[2].

The spin-polarized density functional theory (DFT) calculations have been conducted on Vienna ab-initio simulation package (VASP) to study the alkaline hydrogen evolution reaction.[3, 4] The Projector augmented wave method with a cutoff energy of 400 eV accompanied by Perdew-Burke-Ernzerhof functional has been used in the DFT calculations.[4, 5] DFT-D3 method has been used to correct van der Waals interactions.[6] Four layers of Pt (111) facet have been cleaved with a vacuum layer of 15 Å to build the slab models and the bottom two layers have been fixed to simulate the bulk phase. All models have been fully relaxed with the energy convergence criterion of 10^{-5} eV and the force convergence criterion of 0.02 eV/Å, respectively. Only Γ point has been used in K-point mesh. To obtain the energy barrier of some key steps, the constrained ab initio molecular dynamics (AIMD) has been used with slow-growth method. At the beginning of MD simulation, models have been heated up to 298 K by velocity scaling over 1.49 ps and then equilibrated at 298 K for 1 ps with a 1-fs time step. The collective variable (CV) is chosen shown in Figure 1 and increases with 0.0005 Å per MD step.

r1: distance between atom1 and atom2
r2: distance between atom2 and atom3
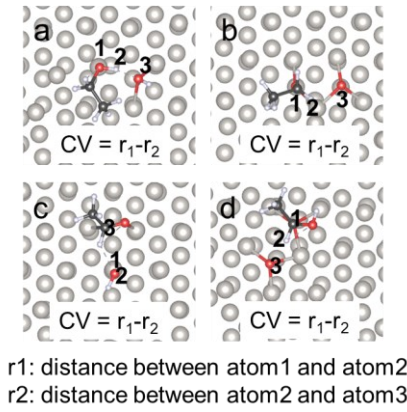
Figure 1 The collective variables used for searching the (a) TS1, (b) TS2, (c) TS3 and (d) TS4 structures, respectively

The adsorption energy (E_{ads}) has been calculated using formula 1,

$$E_{ads} = E_{total} - E_{substrate} - E_{adsorbate} \quad (1)$$

The E_{total}, $E_{substrate}$ and $E_{adsorbate}$ represent the energy of adsorption structure, substrate and adsorbate, respectively. The free energies have been calculated using the following formula 2,

$$G = E_{DFT} + ZPE - TS \quad (2)$$

The G, E_{DFT}, ZPE and TS represent the free energy, energy from DFT calculations, zero point energy and entropic contributions, respectively.

The spin-polarized density functional theory (DFT) calculations have been conducted on Vienna ab-initio simulation package (VASP) to study the ethanol oxidation to acetic acid reaction[3, 4]. The Projector augmented wave method[4] with a cutoff energy of 400 eV accompanied by Perdew-Burke-Ernzerhof functional[5] has been used in the DFT calculations. DFT-D3 method[6] has been used to correct van der Waals interactions. To simulate the reaction in water solution, 56 water molecules had been put into a cubic box with the length of ~12 Å to promise the density of 1 g cm^{-3}. Other reactants had been chosen and put into water according to the specific reactions. All models have been fully relaxed with the energy convergence criterion of 10^{-5} eV and the force convergence criterion of 0.02 eV/Å, respectively. Only Γ point has been used in K-point mesh. To obtain the energy change of some key steps, the constrained ab initio molecular dynamics (AIMD) has been used with slow-growth method. At the beginning of MD simulation, models have been heated up to 298 K by velocity scaling over 1.49 ps and then equilibrated at 298 K for 1 ps with a 1-fs time step. The collective variable (CV) is chosen from the combination of key atom distances in target reactions and increases with 0.0005 Å per MD step.

2. Results and Discussion
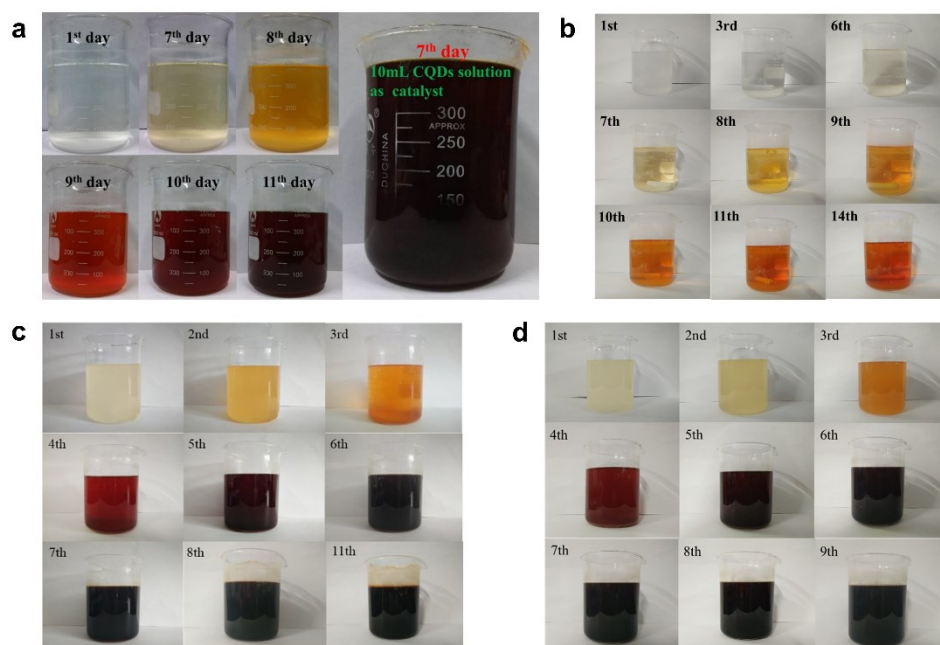
Figure S1. a) Color change of 1.5 M sodium hydroxide dissolved in ethanol and left to stand for 11 days. b) Color change of 1 M sodium hydroxide dissolved in ethanol and left to stand for 14 days. c) Color change of 2.5 M sodium hydroxide dissolved in ethanol and left to stand for 11 days. d) Color change of 3 M sodium hydroxide dissolved in ethanol and left to stand for 9 days. All the solution were placed at room temperature.
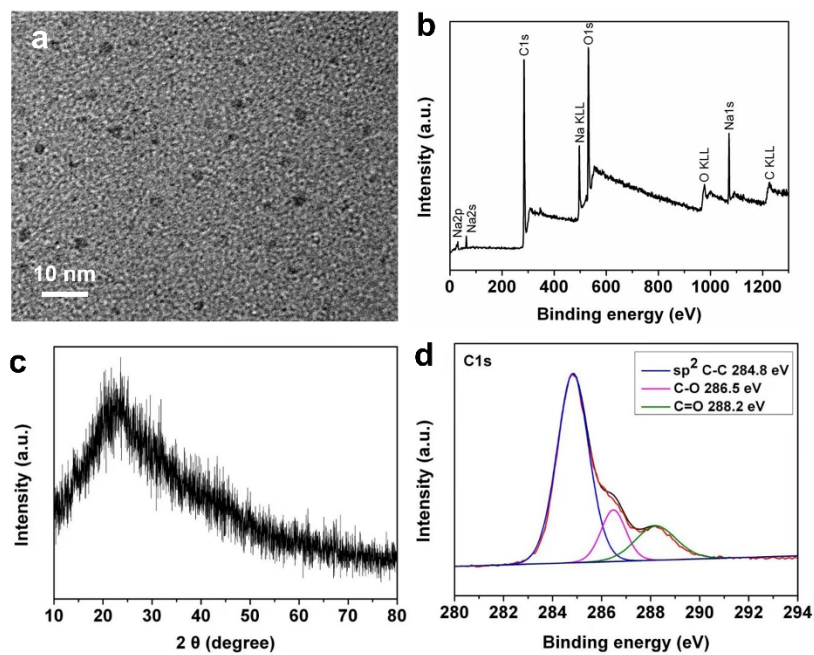
Figure S2. Various characterizations of CDs obtained from 1.5 M sodium hydroxide ethanol solution after lefting to stand for 11 days at room temperature. a) TEM image. b, XPS survey spectrum and d) C1s spectrum. c) XRD pattern.
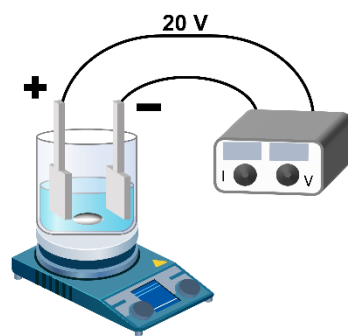
Figure S3. Electrochemical synthesis of carbon dots.

Figure S4. Color change of 8 g NaOH dissolved in 100 mL ethanol (CH_3CH_2OH) under constant stirring with 20V DC voltage at different reaction times (min).
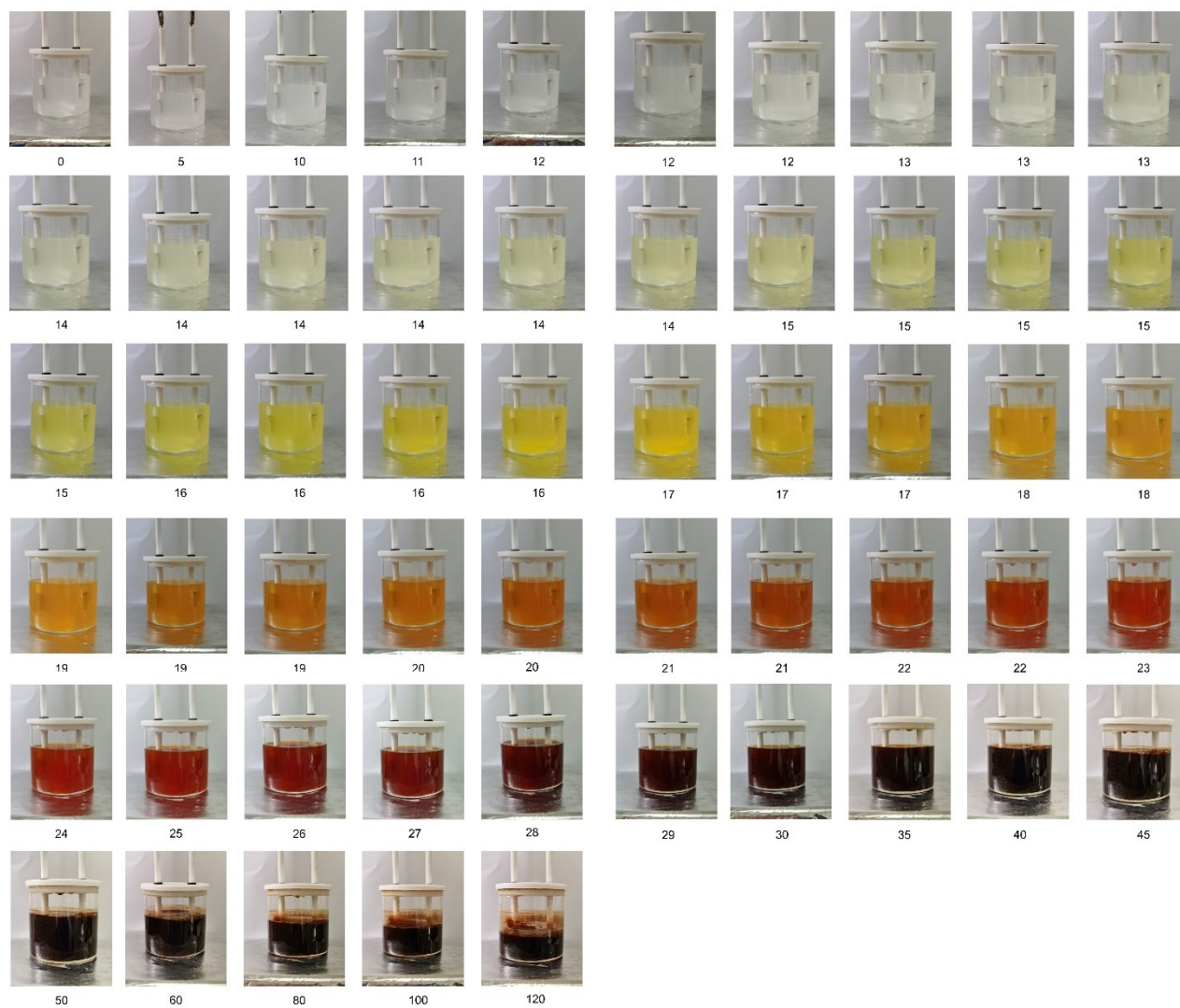
Figure S5. Color change of 8 g NaOH dissolved in the mixture of 90 mL ethanol (CH_3CH_2OH) and 10 mL H_2O under constant stirring with 20V DC voltage at different reaction times (min).
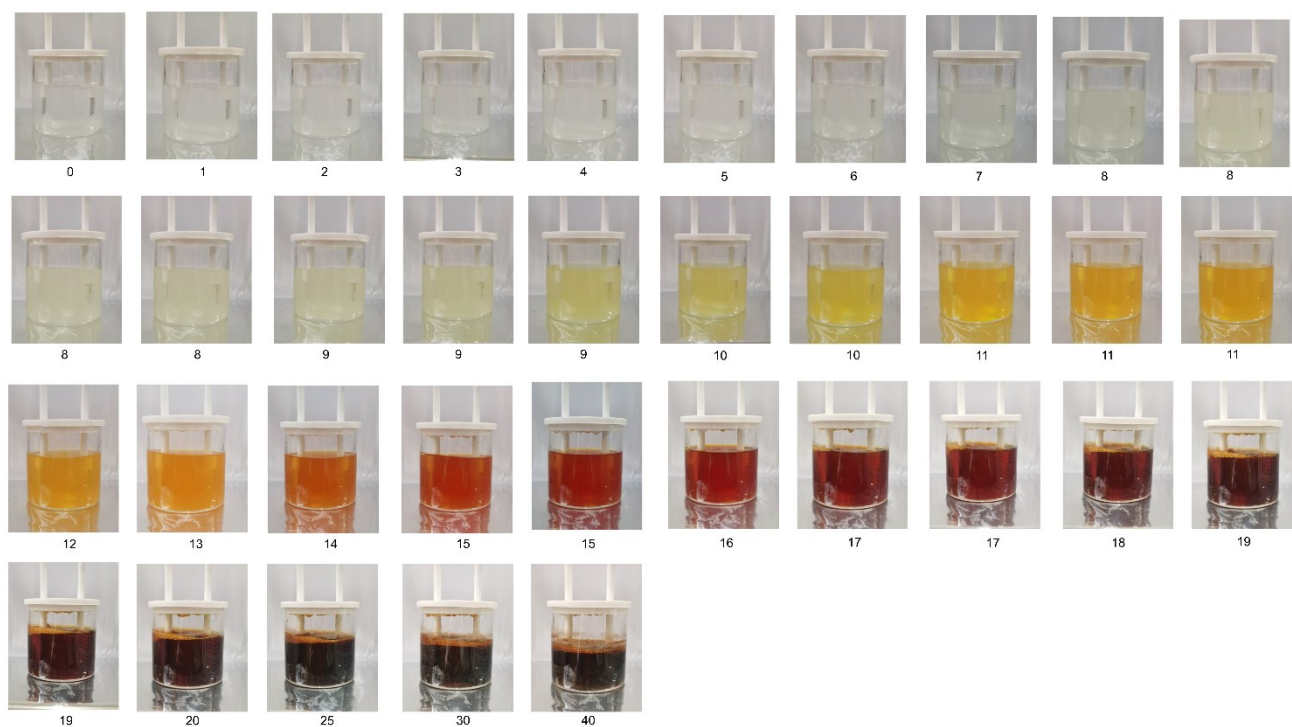
Figure S6. Color change of 8 g NaOH dissolved in the mixture of 80 mL ethanol (CH_3CH_2OH) and 20 mL H_2O under constant stirring with 20 V DC voltage at different reaction times (min).
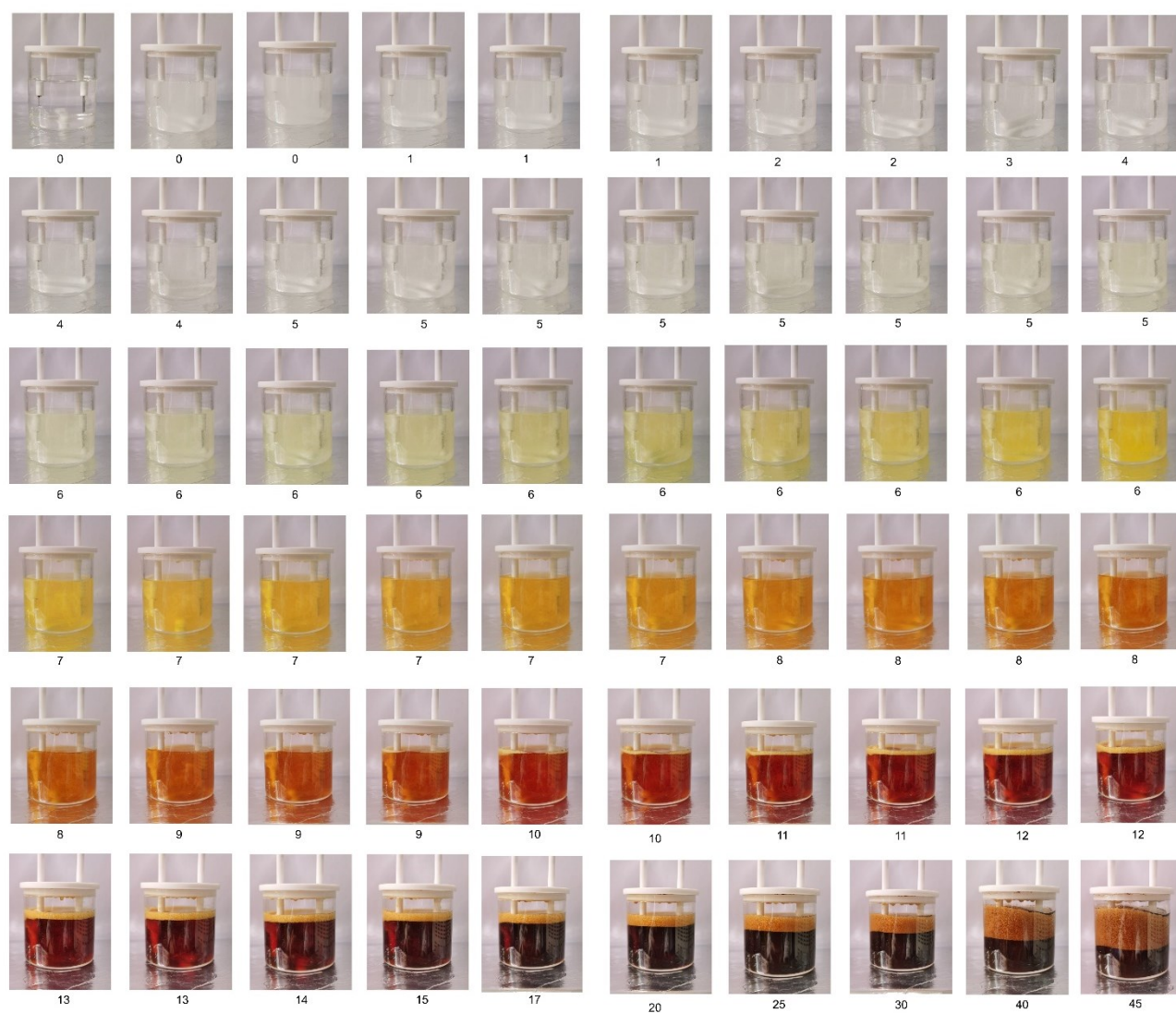
Figure S7. Color change of 8 g NaOH dissolved in the mixture of 60 mL ethanol (CH_3CH_2OH) and 40 mL H_2O under constant stirring with 20 V DC voltage at different reaction times (min).
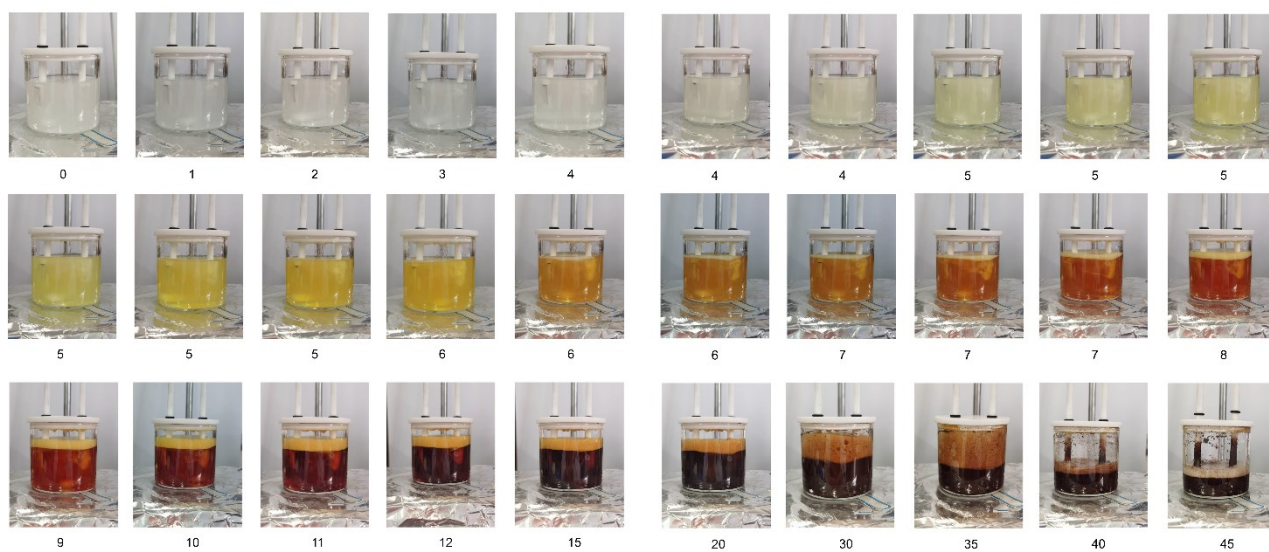
Figure S8. Color change of 8 g NaOH dissolved in the mixture of 50 mL ethanol (CH₃CH₂OH) and 50 mL H₂O under constant stirring with 20 V DC voltage at different reaction times (min).

Figure S9. Color change of 8 g NaOH dissolved in 100 mL ethylene glycol ($C_2H_6O_2$) under constant stirring with 20 V DC voltage at different reaction times (min).
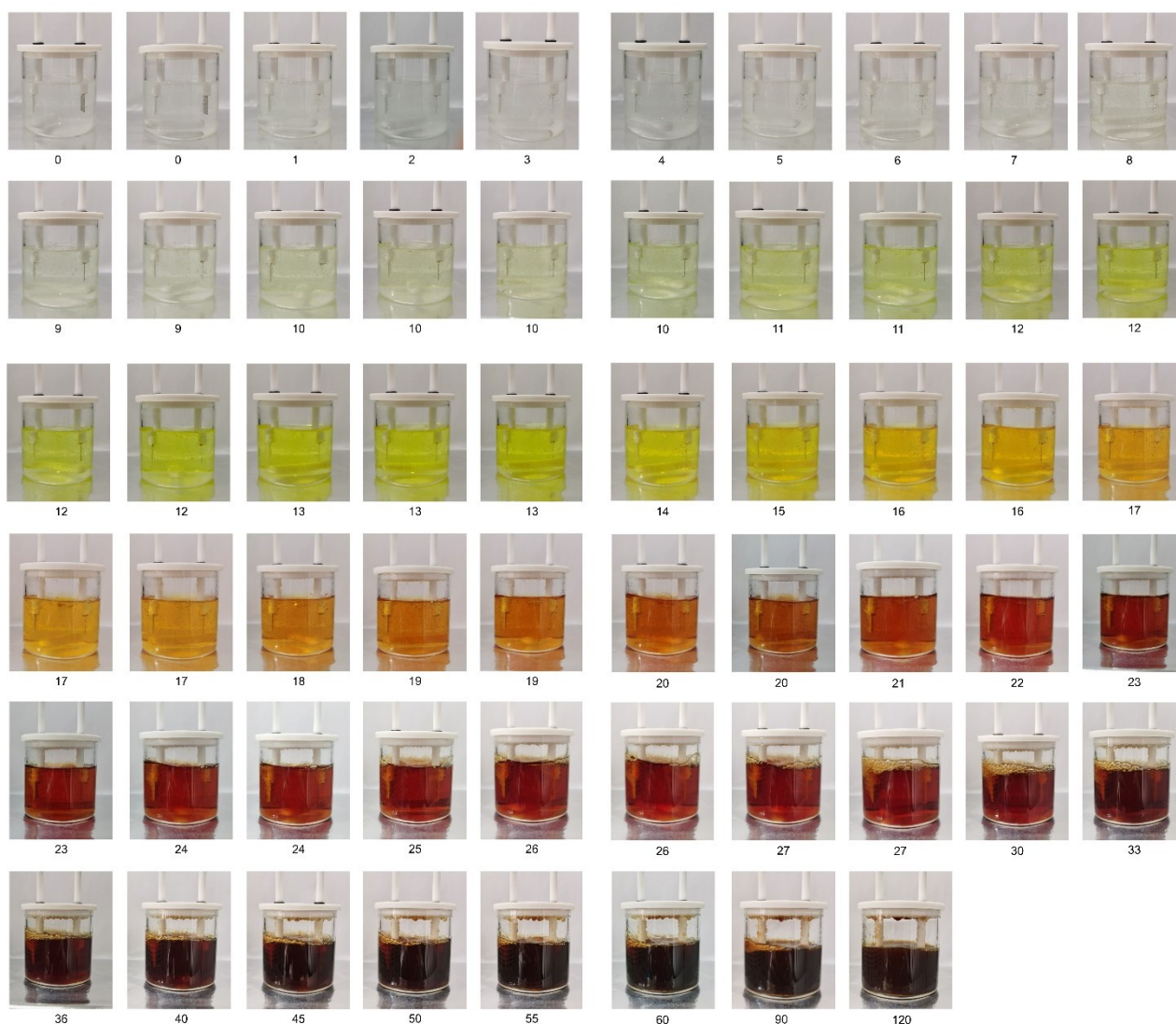
Figure S10. Color change of 8 g NaOH dissolved in the mixture of 80 mL ethylene glycol ($C_2H_6O_2$) and 20 mL H_2O under constant stirring with 20 V DC voltage at different reaction times (min).
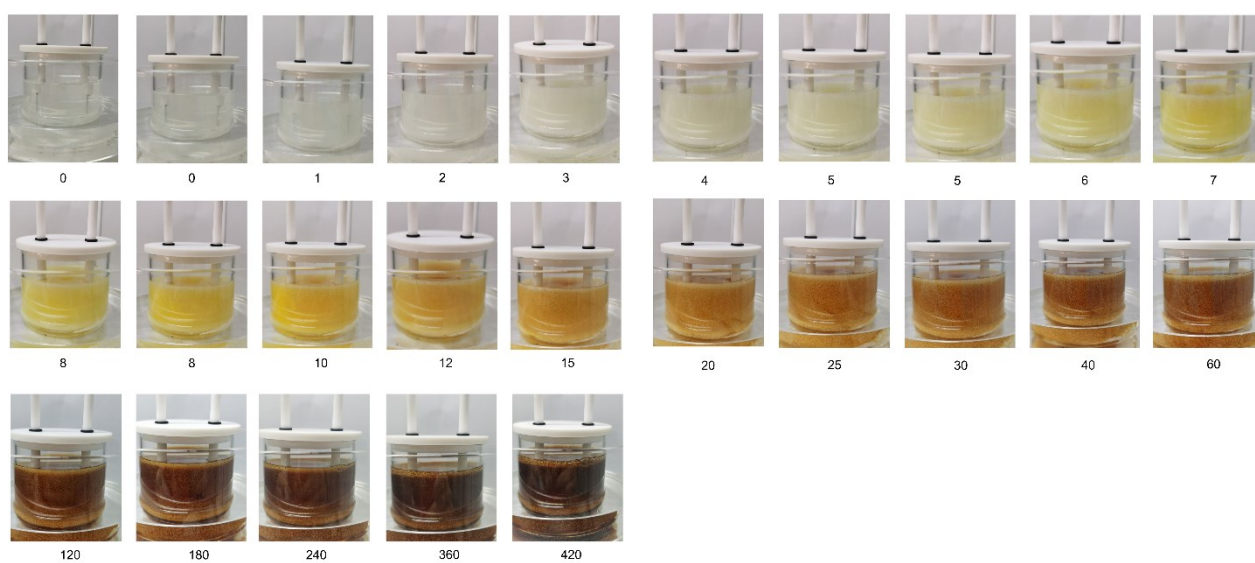
Figure S11. Color change of 8 g NaOH dissolved in 100 mL glycerol ($C_3H_8O_3$) under constant stirring with 20 V DC voltage at different reaction times (min).
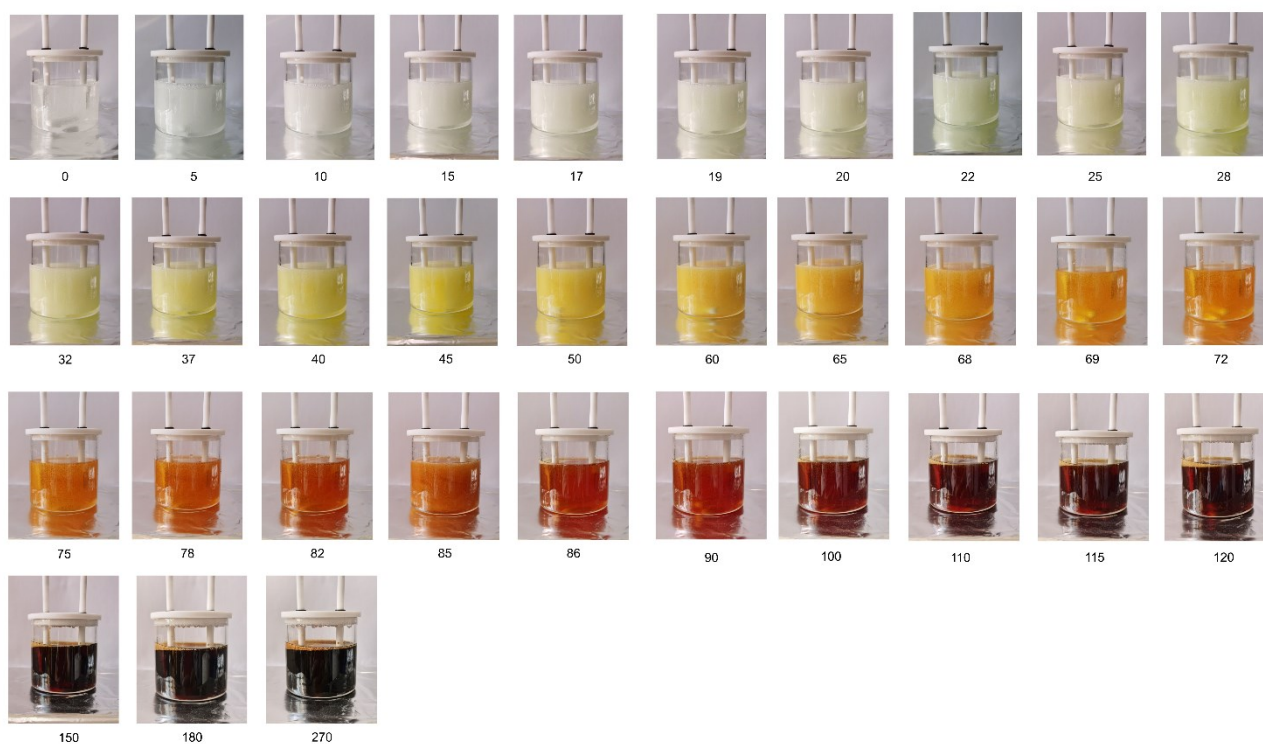
Figure S12. Color change of 8 g NaOH dissolved in the mixture of 80 mL glycerol ($C_3H_8O_3$) and 20 mL H_2O under constant stirring with 20 V DC voltage at different reaction times (min).
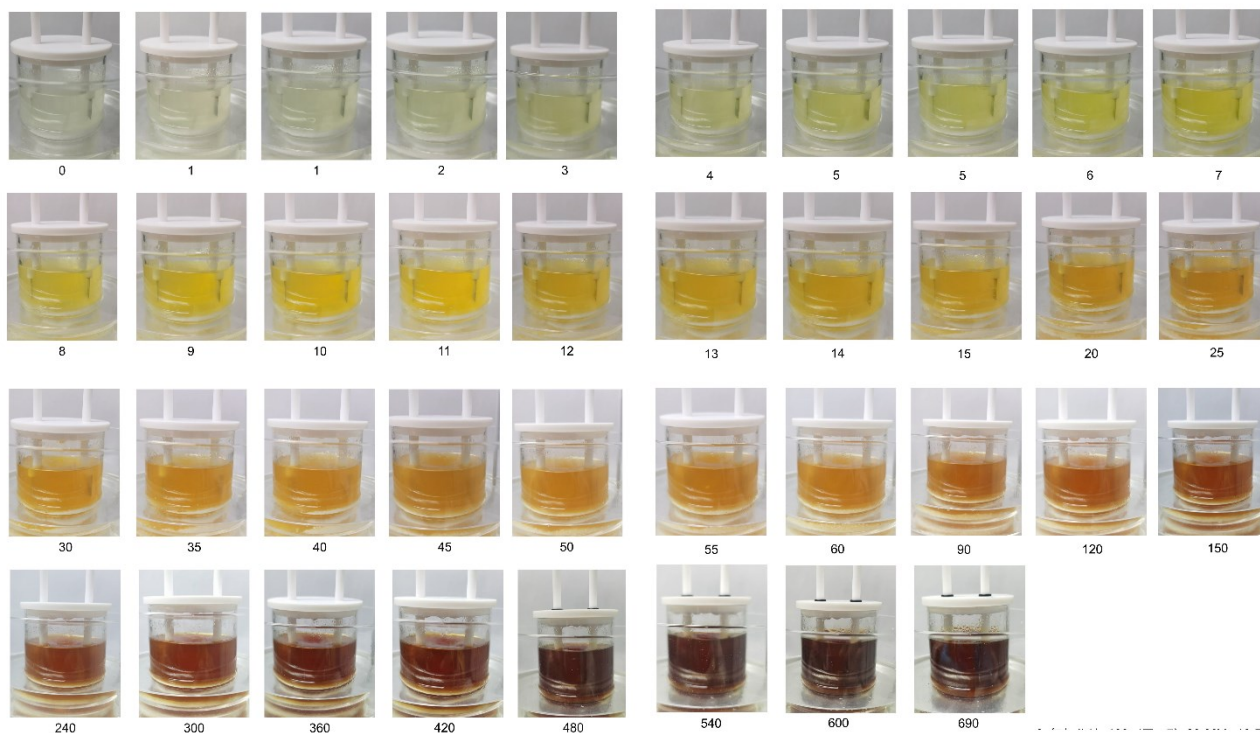
Figure S13. Color change of 8 g NaOH dissolved in 100 mL n-butanol (CH$_3$CH$_2$CH$_2$CH$_2$OH) under constant stirring with 20 V DC voltage at different reaction times (min).
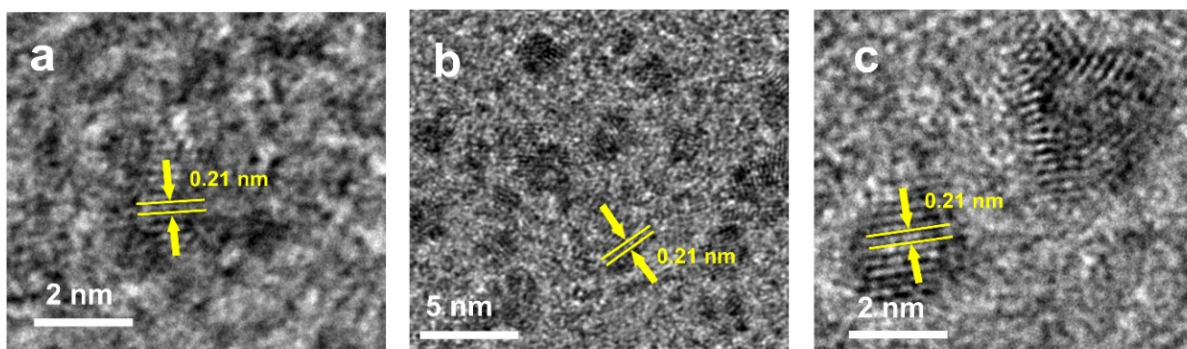
Figure S14. High-resolution (HRTEM) image of an individual a) 100EA-CDs, b) 100EG-CDs, c) 100GL-CDs.
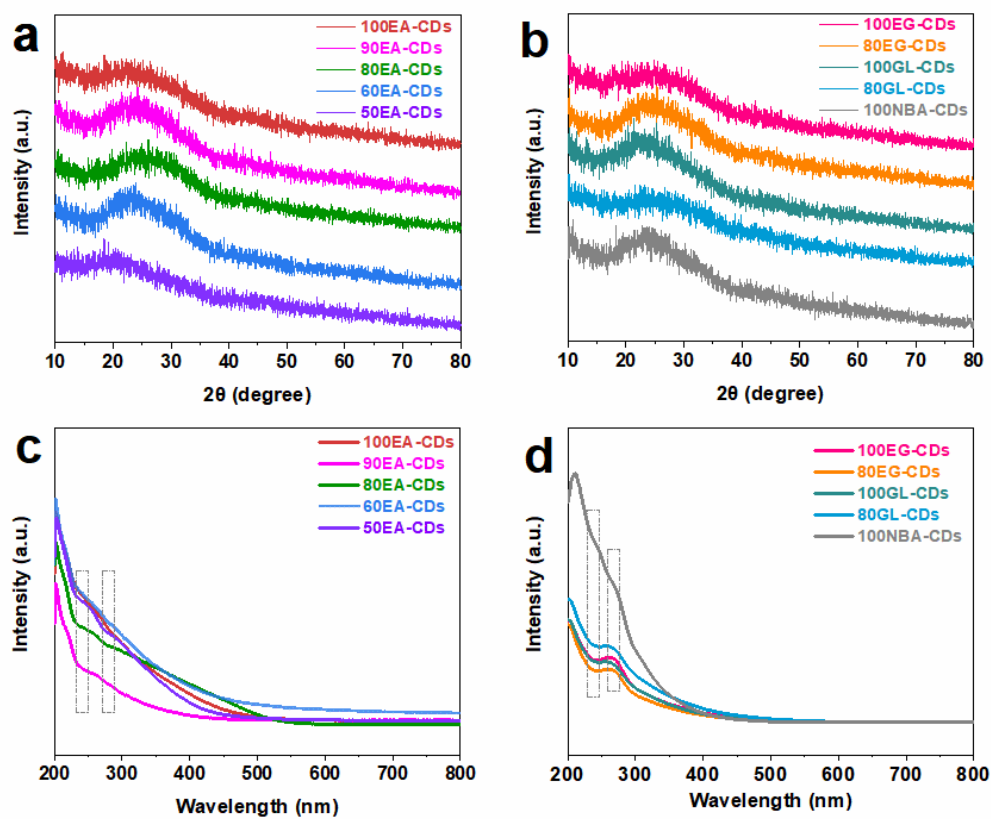
Figure S15. a, b) XRD patterns of different CDs. c, d) UV/Vis absorption spectra of different CDs.
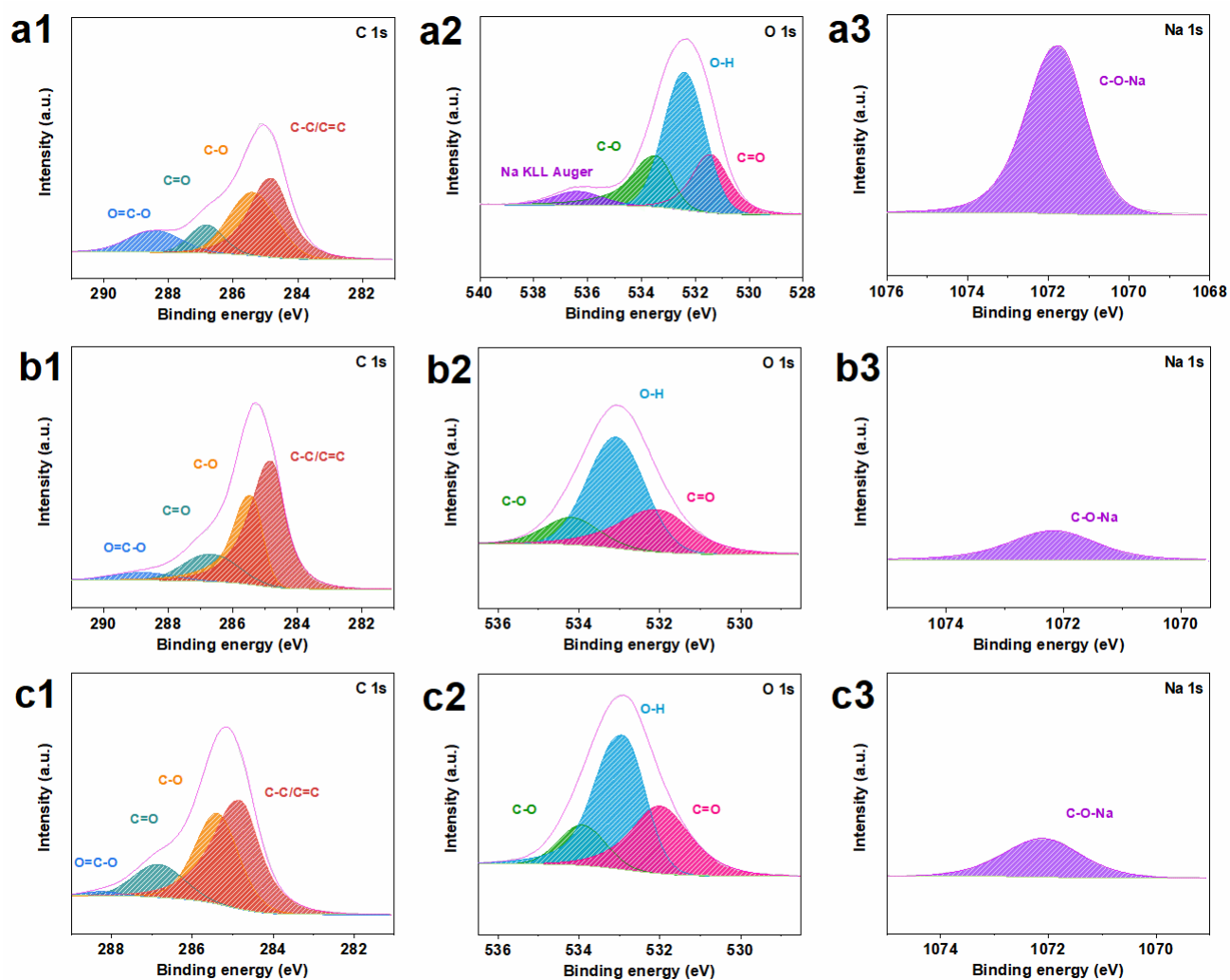
Figure S16. High resolution XPS C 1s (a1), O 1s (a2) and Na 1s (a3) spectra of 100EA-CDs. High resolution XPS C 1s (b1), O 1s (b2) and Na 1s (b3) spectra of 90EA-CDs. High resolution XPS C 1s (c1), O 1s (c2) and Na 1s (c3) spectra of 80EA-CDs.
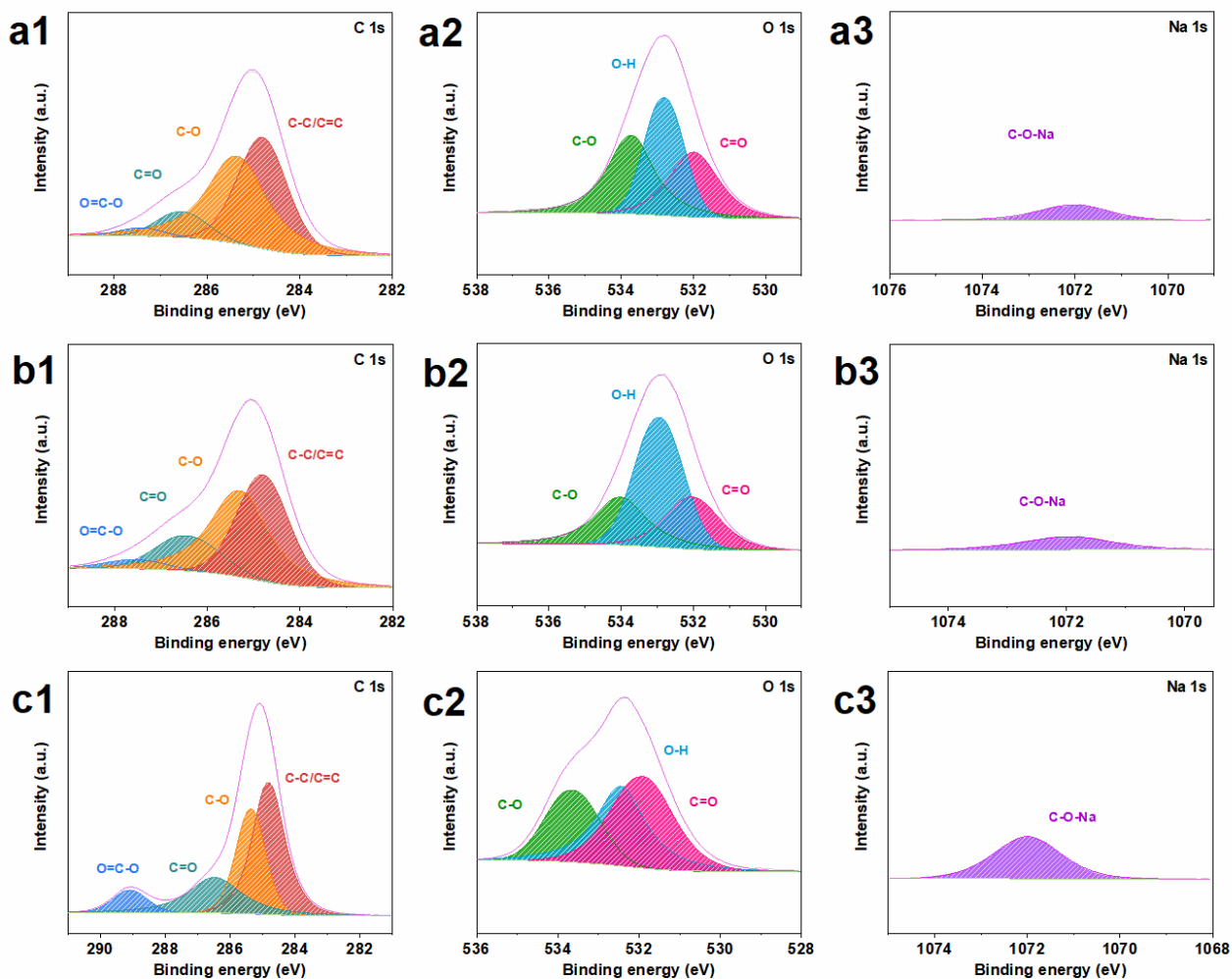
Figure S17. High resolution XPS C 1s (a1), O 1s (a2) and Na 1s (a3) spectra of 60EA-CDs. High resolution XPS C 1s (b1), O 1s (b2) and Na 1s (b3) spectra of 50EA-CDs. High resolution XPS C 1s (c1), O 1s (c2) and Na 1s (c3) spectra of 100NBA-CDs.
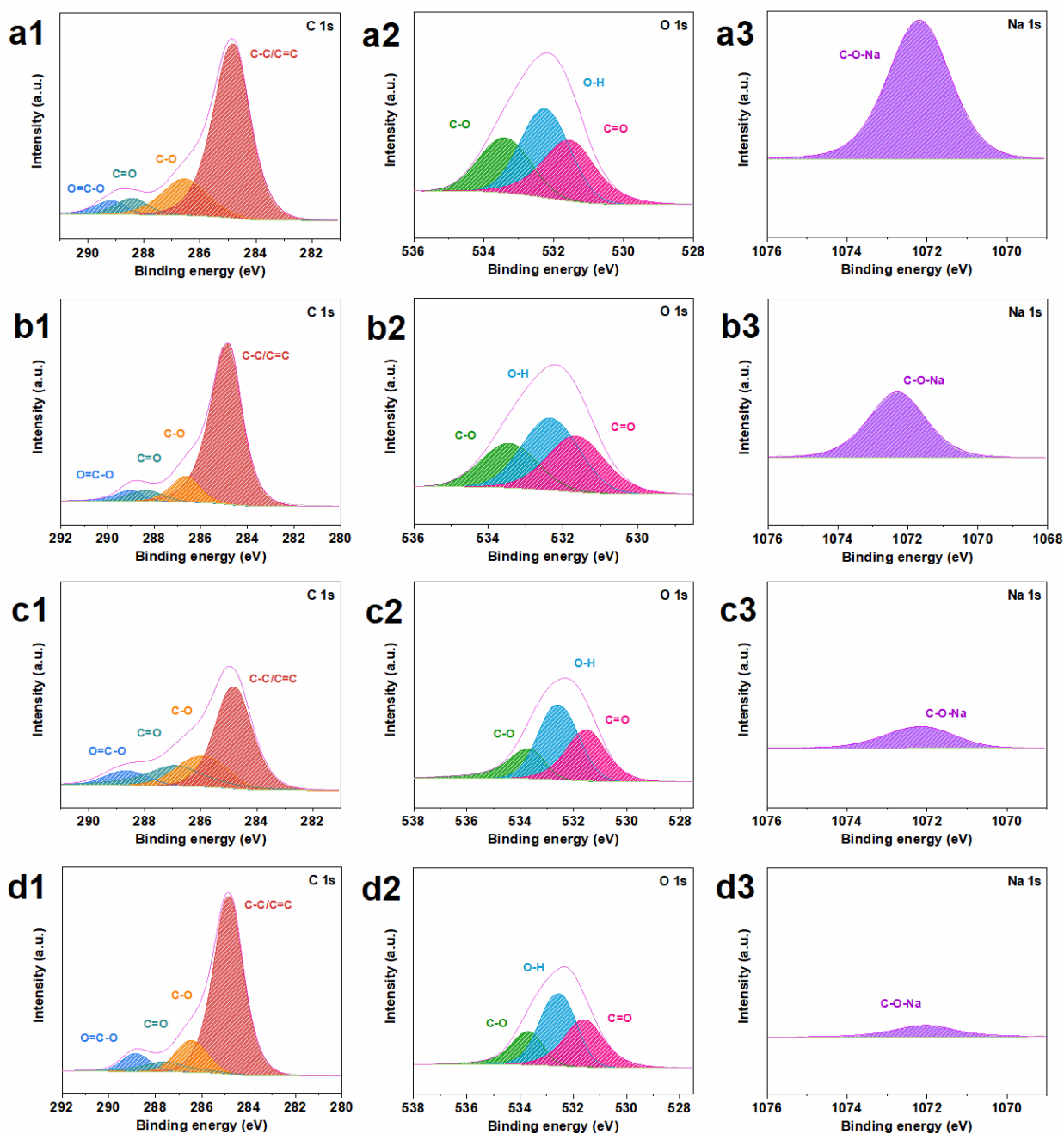
Figure S18. High resolution XPS C 1s (a1), O 1s (a2) and Na 1s (a3) spectra of 100EG-CDs. High resolution XPS C 1s (b1), O 1s (b2) and Na 1s (b3) spectra of 80EG-CDs. High resolution XPS C 1s (c1), O 1s (c2) and Na 1s (c3) spectra of 100GL-CDs. High resolution XPS C 1s (d1), O 1s (d2) and Na 1s (d3) spectra of 80GL-CDs.

a

$CH_3CH_2OH \xrightarrow{\text{NaOH}} CH_3CH_2O^- \xrightarrow[CH_3CHO]{\text{NaOH}} CH_3\overset{\overset{O^-}{|}}{C}HOCH_2CH_3$

$\downarrow CH_3CHO$

$CH_3COOCH_2CH_3 \xleftarrow{\text{NaOH}} CH_3\overset{\overset{|}{O^-}}{C}HO\overset{\overset{|}{CH_3}}{C}HOCH_2CH_3$

b

$CH_3CH_2OH \xrightarrow{CH_3CHO} CH_3\overset{\overset{OCH_2CH_3}{|}}{C}HOCH_2CH_3$

c

$CH_3COOCH_2CH_3 \xrightarrow{\text{NaOH}} CH_3COONa + H_2C=CH_2 + H_2O$

$2CH_3CHO \longrightarrow CH_3\overset{\overset{|}{OH}}{C}HCH_2CHO \longrightarrow CH_3CH=CHCHO \xrightarrow{H_2} CH_3CH=CHCH_2OH \longrightarrow H_2C=CH-CH=CH_2$

$H_2C=CH-CH=CH_2 + H_2C=CH_2 \longrightarrow$ [cyclohexene] $\longrightarrow$ [cyclohexane]

d

CH_3CH_2OH $\xrightarrow{-H}$ CH_3CH_2O $\xrightarrow[]{*O}{-H}$ CH_3CHO
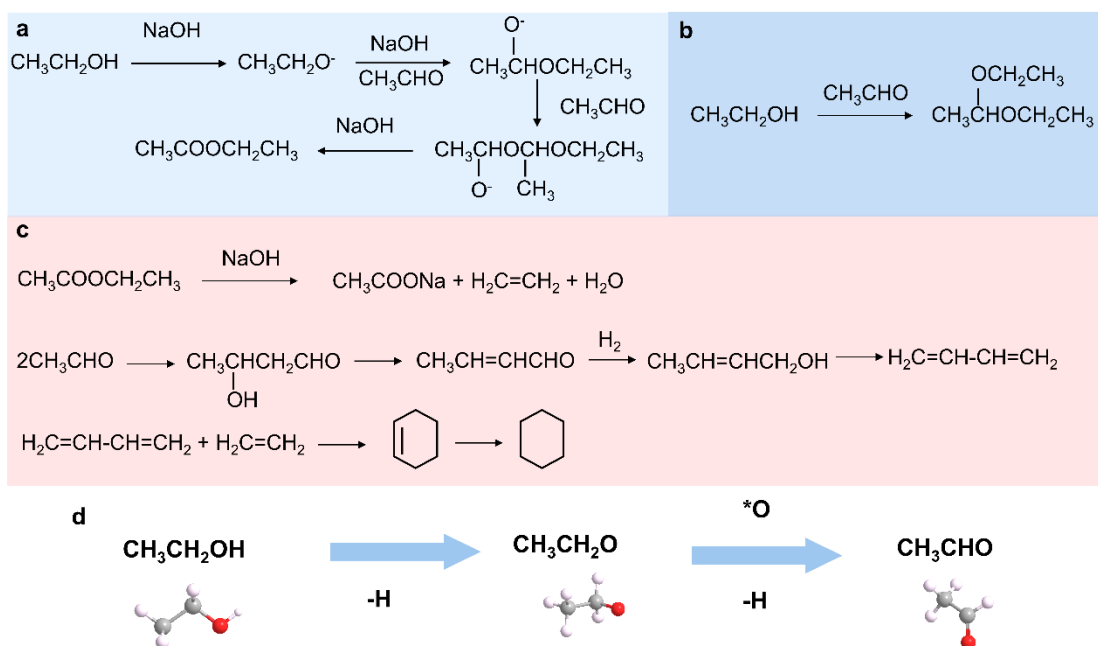
Figure S19. Scope of intermediate products under the strategy; a) ethyl acetate; b) acetal; c) cyclohexane. d) Scheme of the major products involved in the electrochemical synthesis of carbon dots. The gray, red, and white spheres represent C, O, and H atoms, respectively.
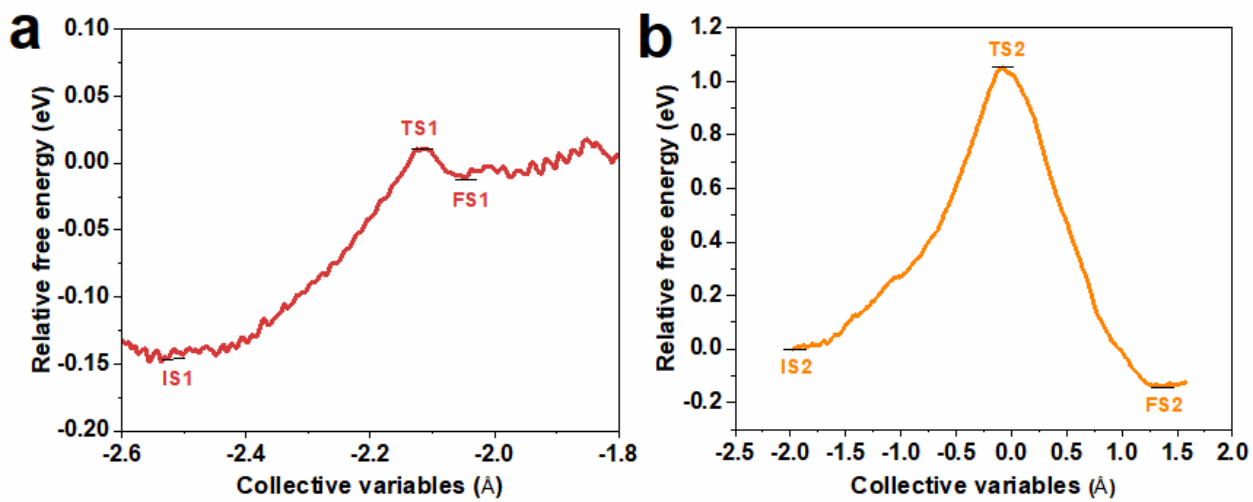
Figure S20. Intermediate process of transition state search.
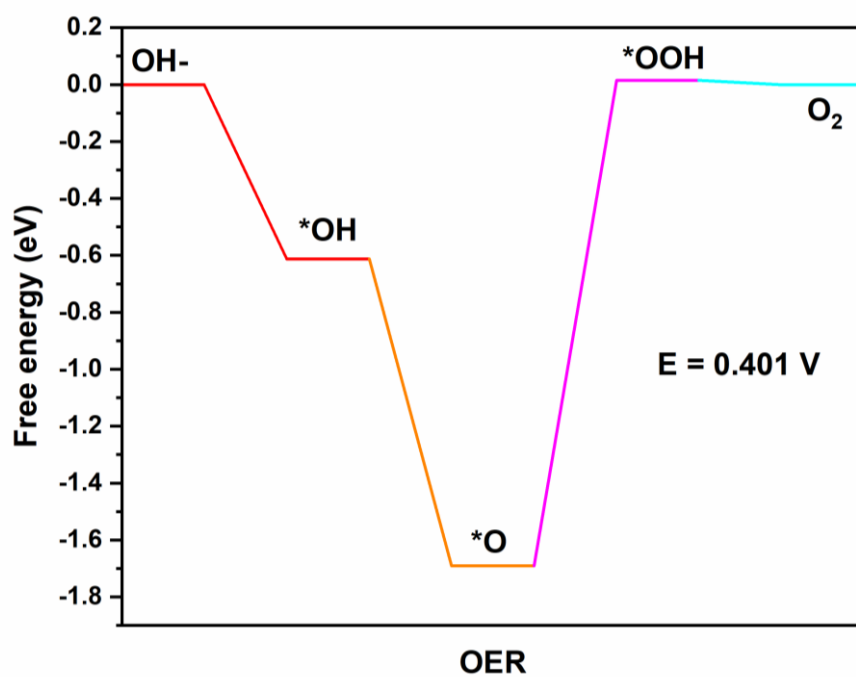
Figure S21. DFT calculated reaction procedure of OER on Pt–Pt sites.
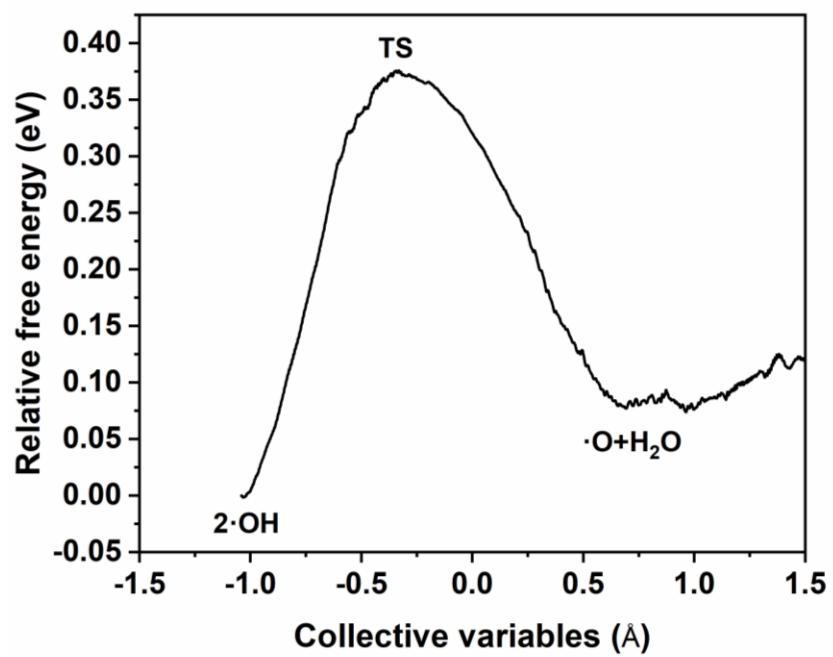
Figure S22. Intermediate process of transition state search between ·OH and ·O.
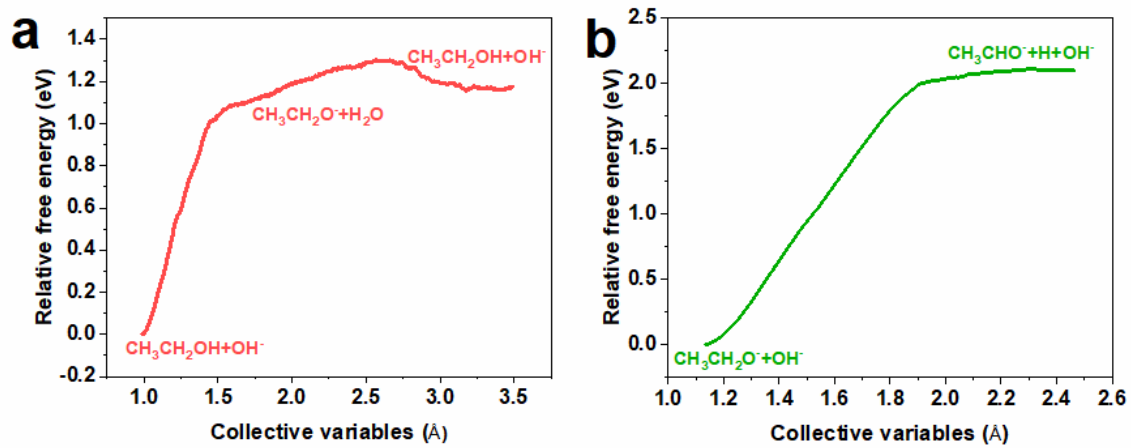
Figure S23. Intermediate process of transition state search.
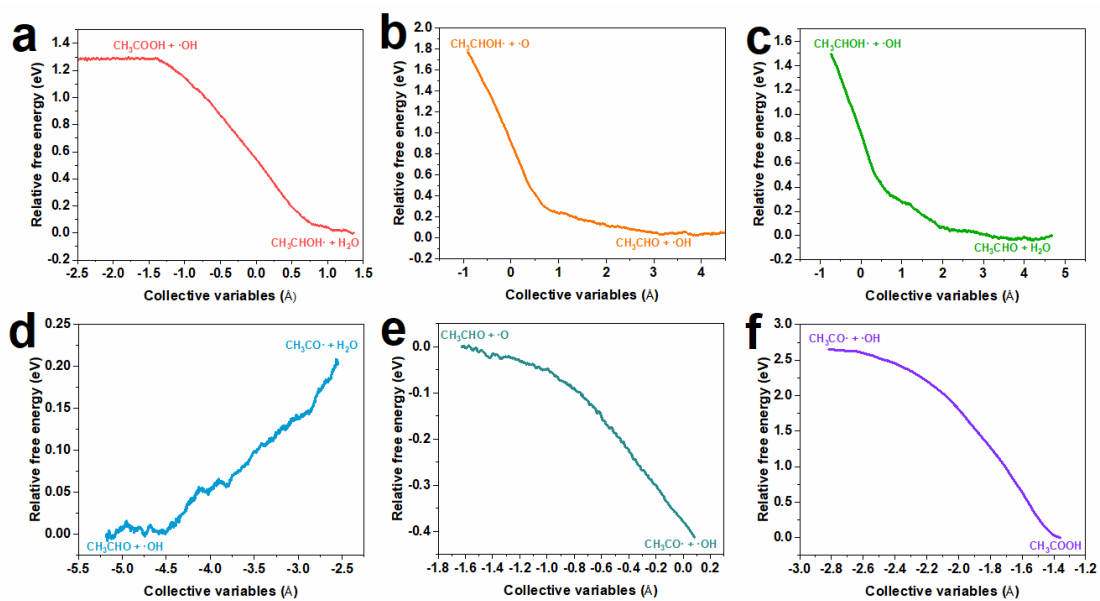
Figure S24. Intermediate process of transition state search.
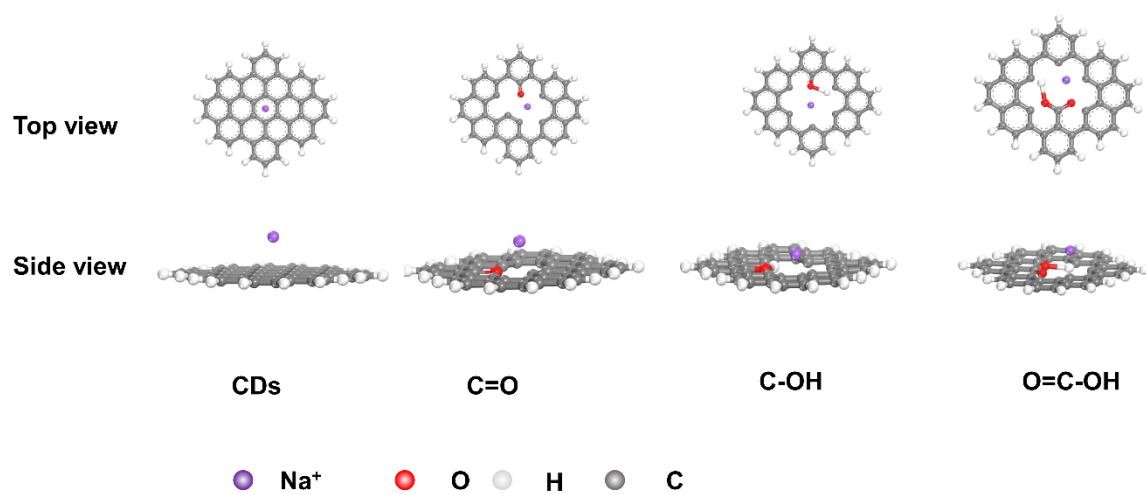
Figure S25. The model structures of binding energy between Na ions and different oxygen functional groups by means of DFT calculation.
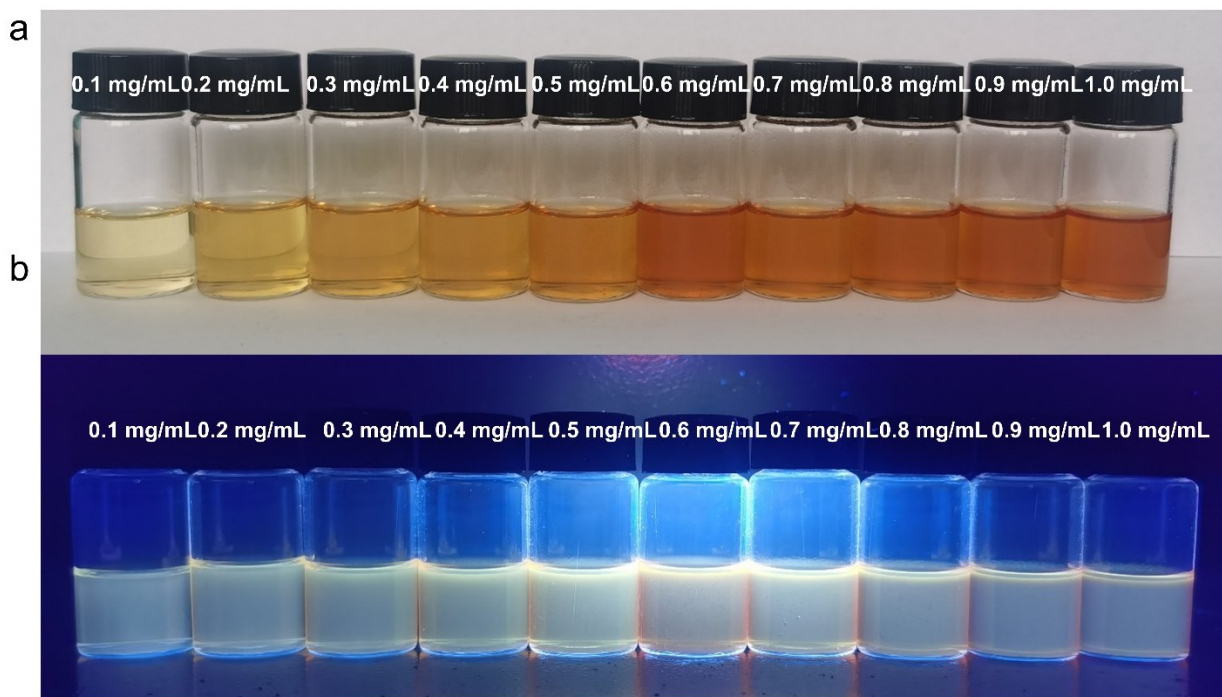
Figure S26. Photographs of Na-CDs dissolved in electrolyte (0.1 mg/mL to 1.0 mg/mL) under sunlight (a), and ultraviolet lamps (b).
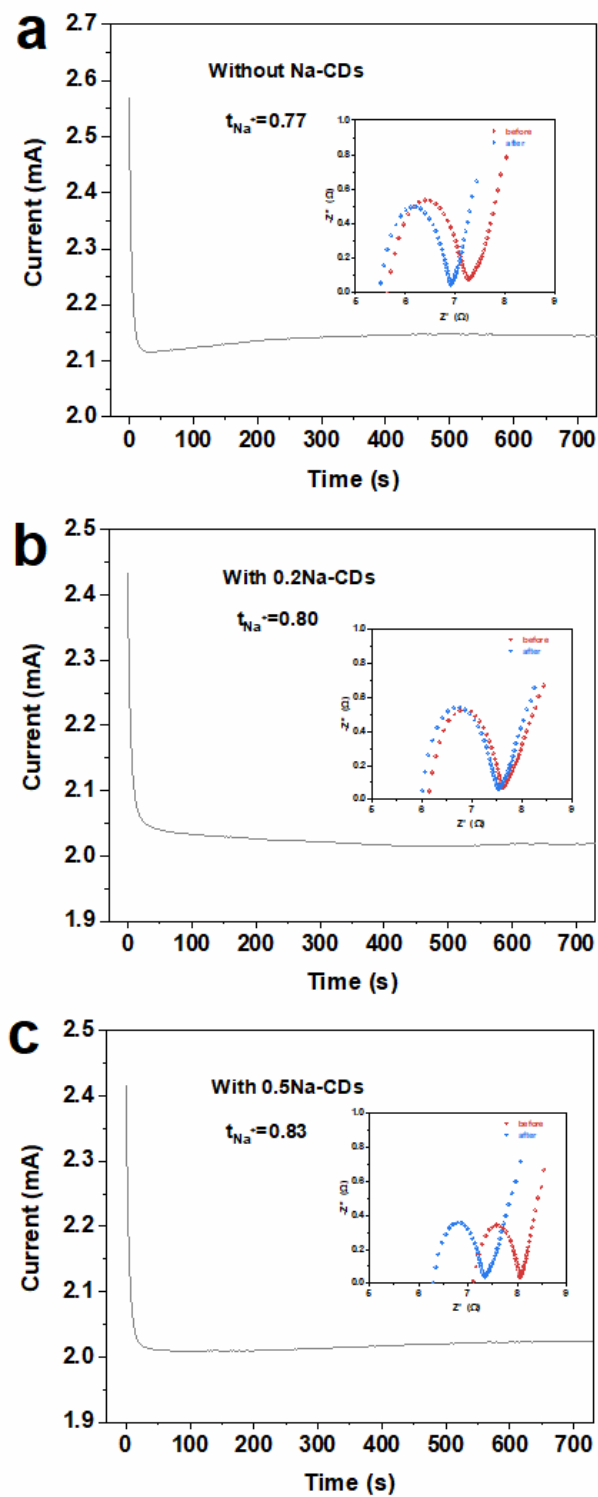
Figure S27. a-c) Current-time curves of Na‖Na symmetric cells in the electrolyte with and without Na-CDs additives at a DC polarization of 20 mV. Inserts are Nyquist plots before and after the DC polarization.
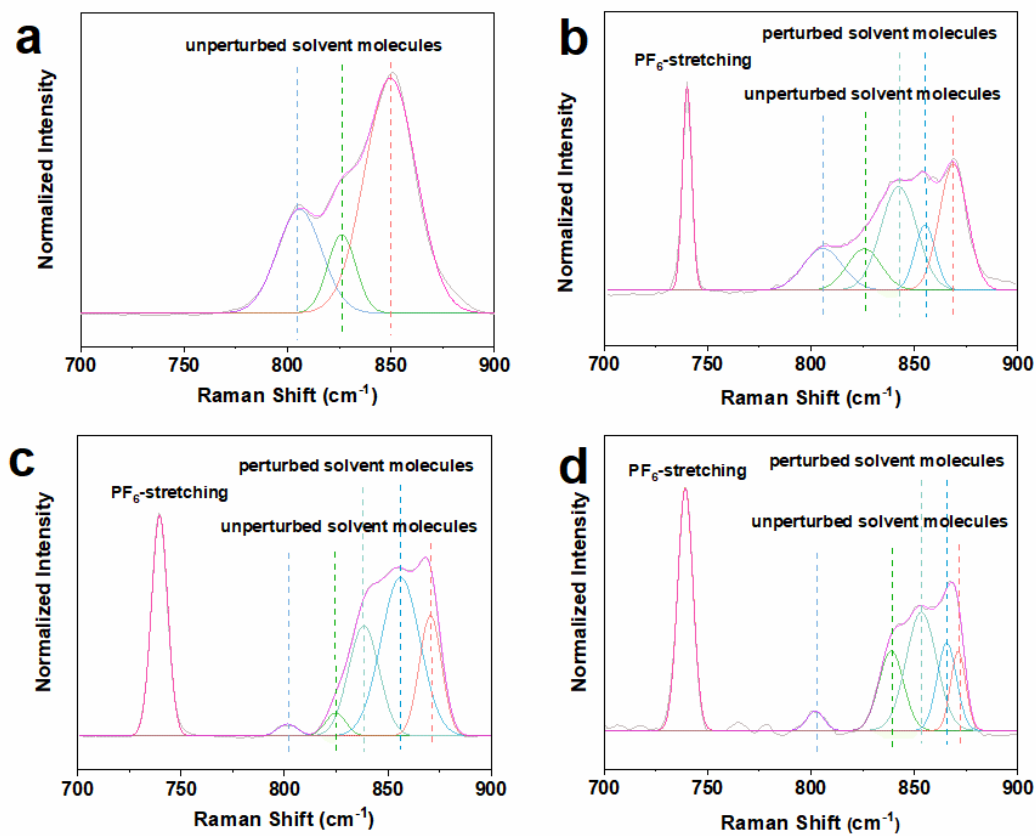
Figure S28. Raman spectra of a) diglyme, b) 1.0 M NaPF$_6$ in DIGLYME electrolyte, c) with 0.2Na-CDs, and d) with 0.5Na-CDs.
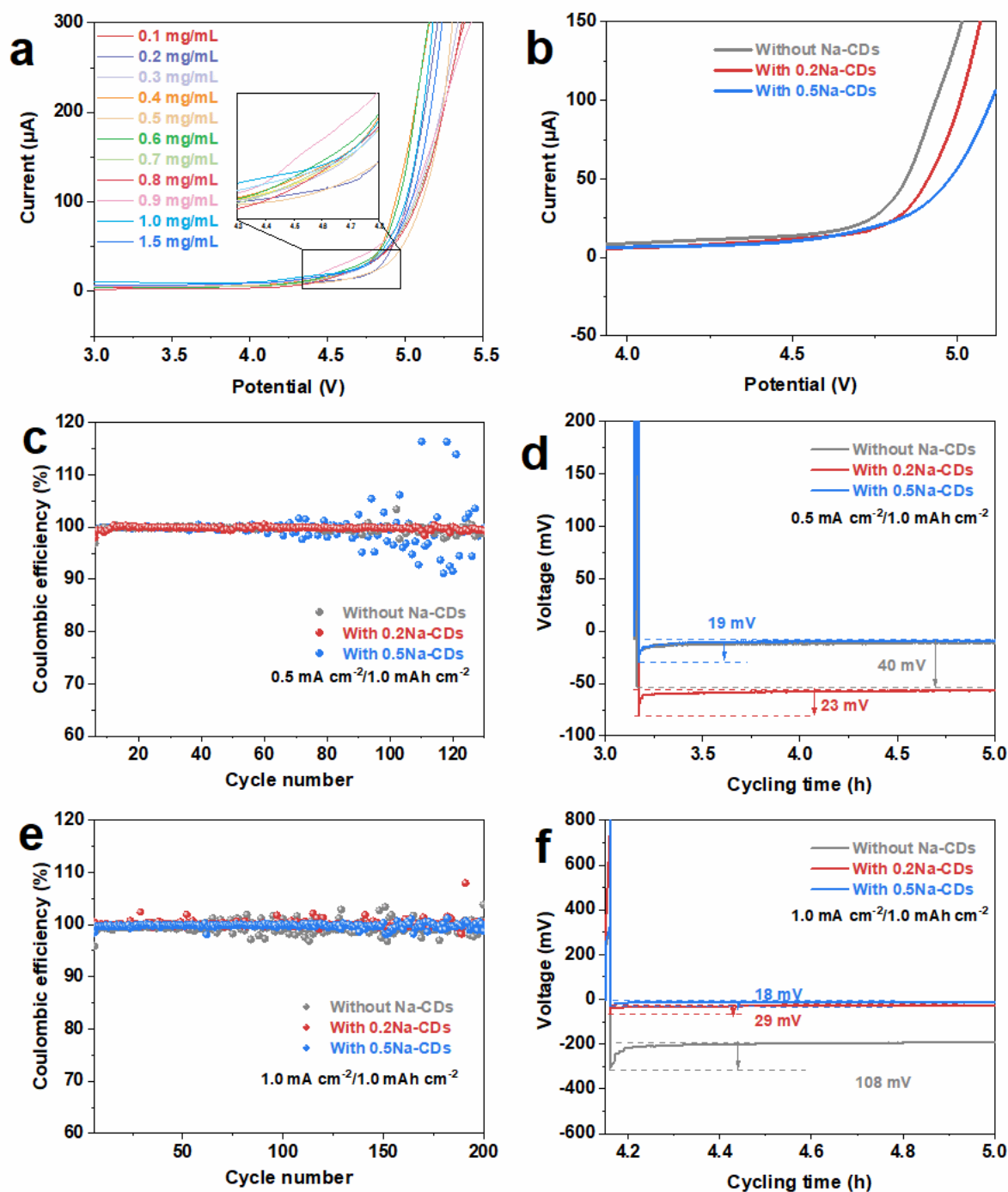
Figure S29. a, b) LSV test of various electrolytes at a scanning rate of 1 mV s^{-1}. Coulombic efficiencies (CE) of Na||Cu cells with and without Na-CDs in 1.0 M NaPF$_6$ in DIGLYME electrolyte cycled under c) 0.5 mA cm^{-2}-1 mAh cm^{-2} and e) 1 mA cm^{-2}-1 mAh cm^{-2}. Charge-discharge voltage curves of Na||Cu cells with and without Na-CDs in 1.0 M NaPF$_6$ in DIGLYME electrolyte cycled under d) 0.5 mA cm^{-2}-1 mAh cm^{-2} and f) 1 mA cm^{-2}-1 mAh cm^{-2}.
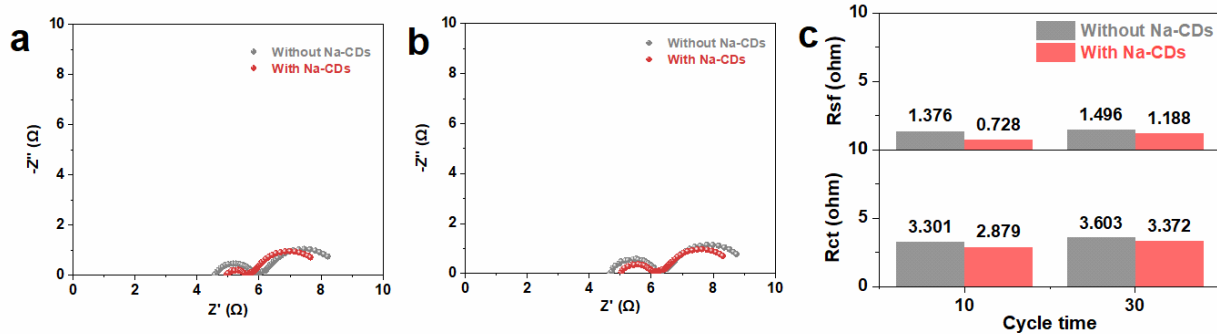
Figure S30. The Nyquist plots of Na‖Na symmetric cells with and without Na-CDs additives at a) 10 cycles and b) 30 cycles with c) their corresponding charge transfer resistance.
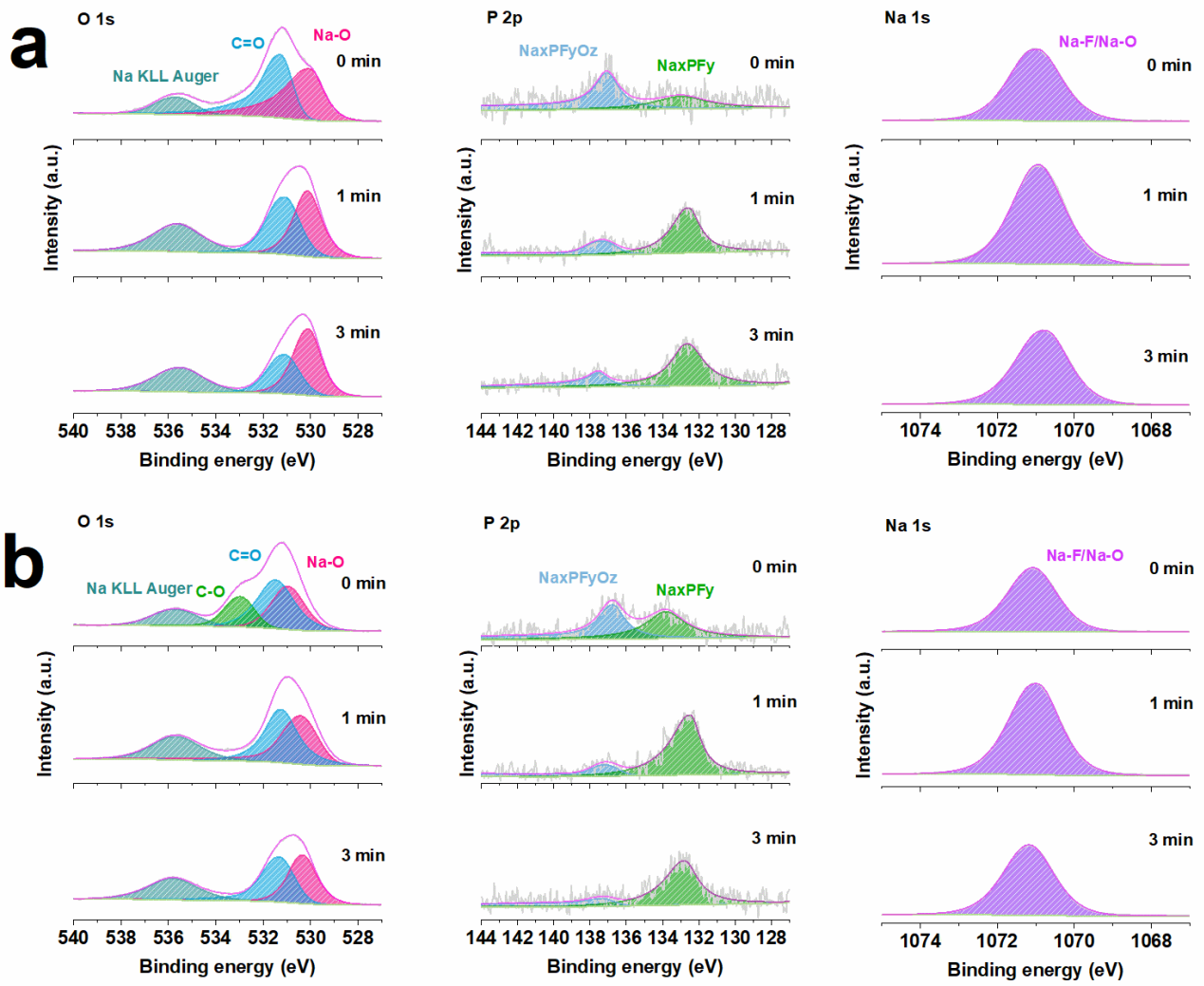
Figure S31. XPS depth profiles of O 1s, P 2p, and Na 1s for Na anode after 10 cycles a) in blank and b) Na-CDs electrolytes.
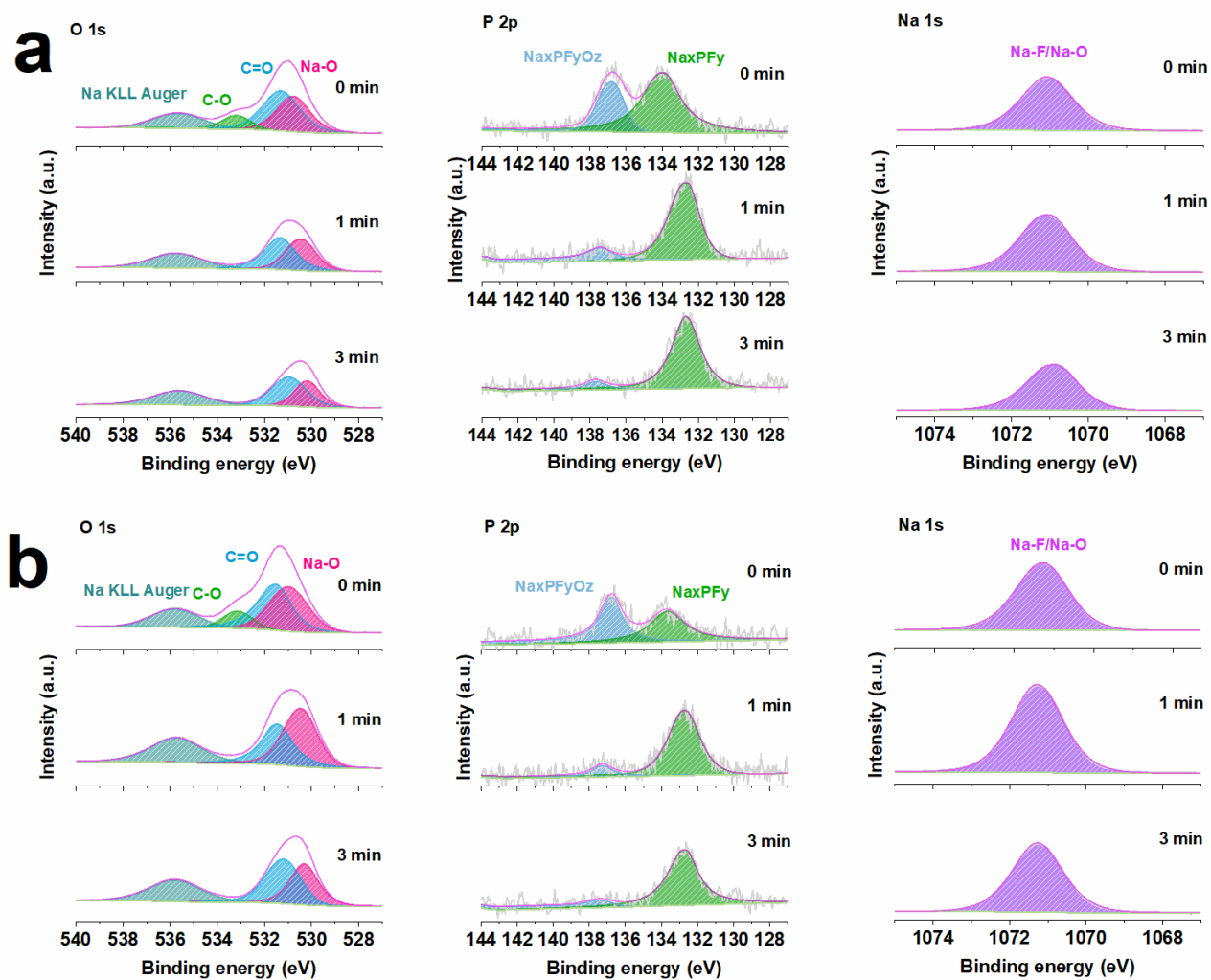
Figure S32. XPS depth profiles of O 1s, P 2p, and Na 1s for Na anode after 30 cycles a) in blank and b) Na-CDs electrolytes.
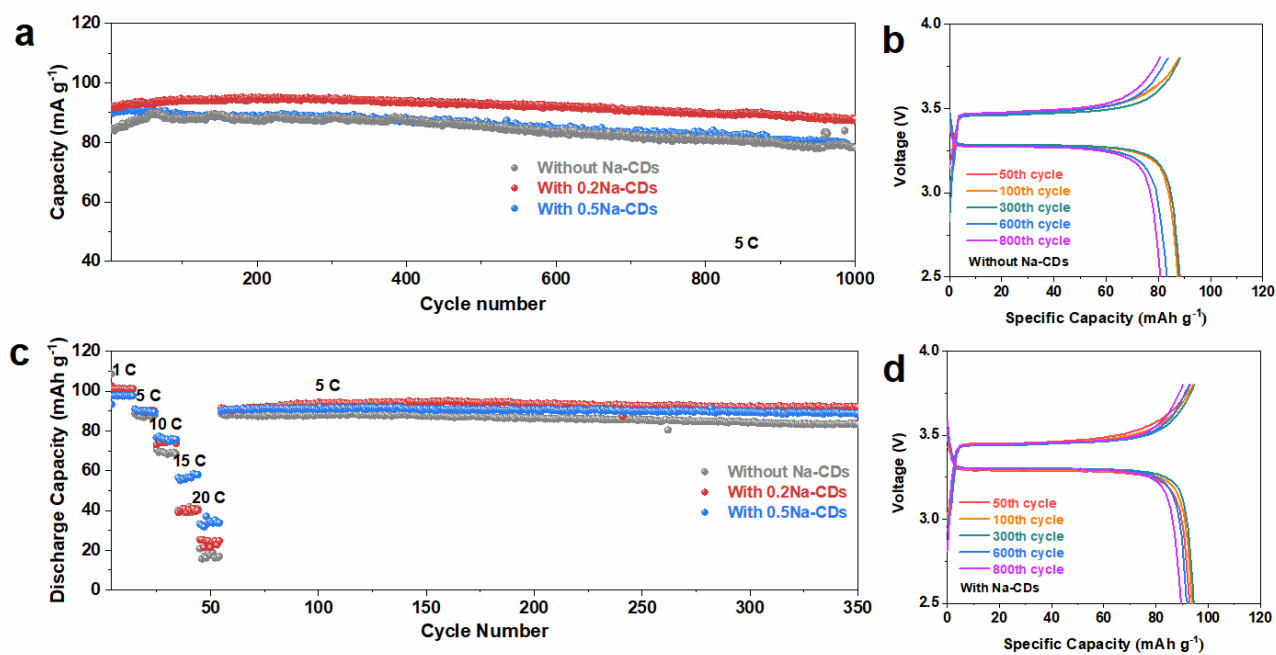
Figure S33. a) Cycling performance of Na||NVP full cells and b, d) the corresponding charge/discharge curves with and without Na-CDs. c) Rate performance of Na||NVP full cells with and without Na-CDs.
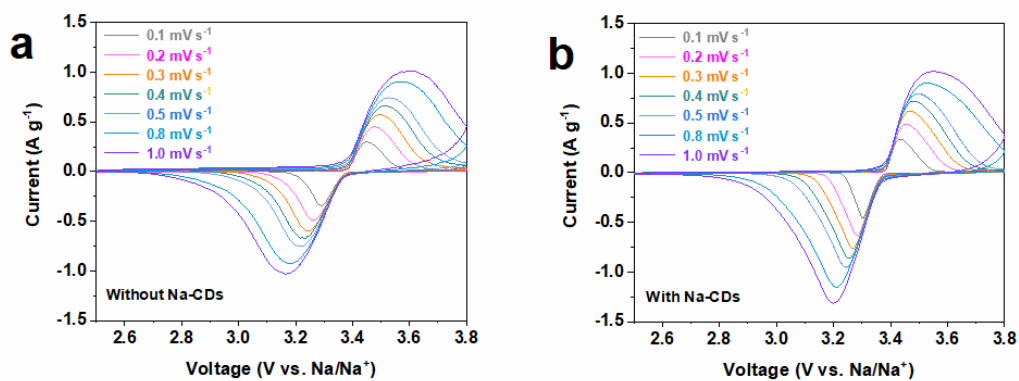
Figure S34. a) Cyclic voltammetry (CV) curves of Na||NVP full cells with and without Na-CDs at scan rates of 0.1 - 1.0 mV s^{-1}.

3. References

1. D. Wang, P. Cai, G.-Q. Zou, H.-S. Hou, X.-B. Ji, Y. Tian and Z. Long, Ultra-stable carbon-coated sodium vanadium phosphate as cathode material for sodium-ion battery, *Rare Metals*, 2022, **41**, 115-124.
2. D. Hong, Y. Choi, J. Ryu, J. Mun, W. Choi, M. Park, Y. Lee, N.-S. Choi, G. Lee, B.-S. Kim and S. Park, Homogeneous Li deposition through the control of carbon dot-assisted Li-dendrite morphology for high-performance Li-metal batteries, *Journal of Materials Chemistry A*, 2019, **7**, 20325-20334.
3. Kresse and Furthmuller, Efficient iterative schemes for ab initio total-energy calculations using a plane-wave basis set, *Physical review. B, Condensed matter*, 1996, **54**, 11169-11186.
4. D. Joubert, - From ultrasoft pseudopotentials to the projector augmented-wave method, 1999, **- 59**, - 1775.
5. K. Burke and M. Ernzerhof, - Generalized Gradient Approximation Made Simple, 1996, **- 77**, - 3868.
6. S. Grimme, J. Antony, S. Ehrlich and H. Krieg, A consistent and accurate ab initio parametrization of density functional dispersion correction (DFT-D) for the 94 elements H-Pu, *Journal of Chemical Physics*, 2010, **132**.